JOURNAL OF MOLECULAR SPECTROSCOPY 169, 268–285 (1995)

Fourier Transform Infrared Emission Spectroscopy of a New $b^3\Pi$–$a^3\Delta$ System of HfO

R. S. RAM AND P. F. BERNATH

Department of Chemistry, University of Arizona, Tucson, Arizona 85721; and Department of Chemistry, University of Waterloo, Waterloo, Ontario, Canada N2l 3G1

The emission spectrum of HfO has been investigated in the 400 nm to 5 μm spectral region with a Fourier transform spectrometer. The bands were excited in a hafnium hollow cathode lamp in the presence of neon and a trace of oxygen. In the 6900–8000 cm^{-1} region, four new sequences of bands were observed with the 0–0 Q heads at 7060 cm^{-1}, 7355.4 cm^{-1}, 7376.8 cm^{-1}, and 7929.5 cm^{-1}. These bands have been identified as the $^3\Pi_{0^+}$–$^3\Delta_1$, $^3\Pi_{0^-}$–$^3\Delta_1$, $^3\Pi_1$–$^3\Delta_2$ and $^3\Pi_2$–$^3\Delta_3$ subbands of the $b^3\Pi$–$a^3\Delta$ transition. The rotational analysis of the 0–0 and 1–1 bands of each subband has been performed and the equilibrium rotational constants for each spin component of the $b^3\Pi$ and $a^3\Delta$ states have been obtained.

INTRODUCTION

Diatomic transition metal oxides have been the subject of numerous spectroscopic investigations due to their important role in chemistry and astrophysics (*1–3*). Some of these molecules, for example, TiO (*4, 5*) and YO (*6–8*), have been identified in the atmospheres of cool stars and are being used by astronomers in stellar classification (*9*). The transition metal oxides are also important for the theoretical understanding of chemical bonding in simple metal systems.

Over the past decade a great deal of effort has been devoted to the study of transition metal monoxides. As a result the ground states of all 3*d* transition metal monoxides have been characterized. Many excited electronic states of the 3*d* oxides are now also known (*1, 10*). Understanding of the 4*d* transition metal monoxides is more limited; YO (*10–13*), ZrO (*10, 14–18*), NbO (*10, 19*), MoO (*20, 21*), RuO (*10, 22*), and AgO (*10*) are relatively well characterized in this family.

The heavy 5*d* transition metal oxides suffer from an additional complication because strong spin–orbit interactions limit the validity of the S, Σ, and Λ quantum numbers. The large number of unpaired electrons in these metals results in many low-lying electronic states with large spin–orbit intervals. The different spin components of a $^{2S+1}\Lambda$ term are split into widely separated Ω-states with Hund's case (c) electronic structure. The various electronic states and spin components interact with each other and cause perturbations. This leads to difficulty in the interpretation of the observed spectra as well as in the ab initio prediction of the molecular properties. Due to these limitations there are essentially no ab initio predictions and only limited experimental (*10, 23–30*) data are available for the 5*d* series of transition metal oxides.

The infrared electronic transitions of transition metal oxides are expected to be relatively free of perturbations because of the lower density of states in this energy range. Recently we have successfully applied Fourier transform emission spectroscopy to the study of the near infrared spectra of some transition metal oxides such as PtO (*30*), NiO (*31*), and CoO (*32*). These spectra were free from local perturbations. In

0022-2852/95 $6.00

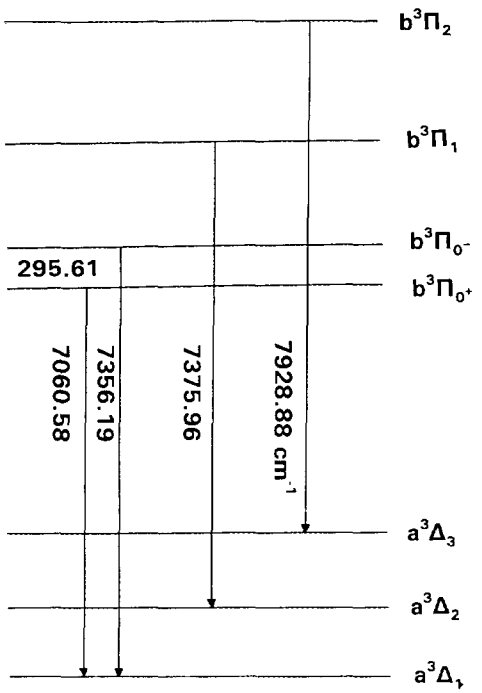

FIG. 1. Energy-level diagram for the $b^3\Pi$–$a^3\Delta$ electronic transition of HfO.

this study we have applied this technique to the study of the near infrared spectra of HfO. The new HfO bands in this region are free from local perturbations, as expected.

The HfO molecule has been known for several decades. This molecule was initially observed by King (*33*) in 1929. Since then there have been several reports on the electronic spectra of this molecule, mainly in the visible region (*34–36*). Gatterer *et al.* (*36*) classified the HfO bands into nine electronic transitions and designated them by the letters *A* to *J*. They noted that six of these transitions, *A*, *B*, *D*, *E*, *F*, and *G*, have the same common lower electronic state. In a later study of this molecule, Weltner and McLeod (*37*) observed the same six electronic transitions in absorption in solid neon and argon matrices and concluded that the ground state of this molecule is a $^1\Sigma^+$ state. This conclusion was consistent with the results obtained for ZrO (*10, 18*). The microwave spectra of HfO, along with those of YO, LaO, and ZrO, have been obtained by Suenram *et al.* (*24*) by coupling a laser ablation source with a pulsed-nozzle Fourier transform microwave spectrometer. In this work the electric dipole moments and nuclear quadrupole coupling constants have been determined for the ground electronic states. The ionization potential and other thermodynamic properties of HfO have been determined by mass spectrometry (*38, 39*). The ionization potential was measured to be 7.55 eV (*38*), while the dissociation energy is 188.9 kcal/mole (*39*).

Edvinsson and Nylén (*40*) have studied the spectra of HfO in the 230–1150 nm spectral region at high resolution using a grating spectrograph and have reported the rotational analysis of nine transitions in the visible region. Six of these transitions have a common lower state, which is the ground state $X\,^1\Sigma^+$. The remaining three transitions do not have any states in common with the known states. These transitions were labelled as $C - x_1$, $J - x_2$, and $H - x_3$ by Huber and Herzberg (*10*). The bands

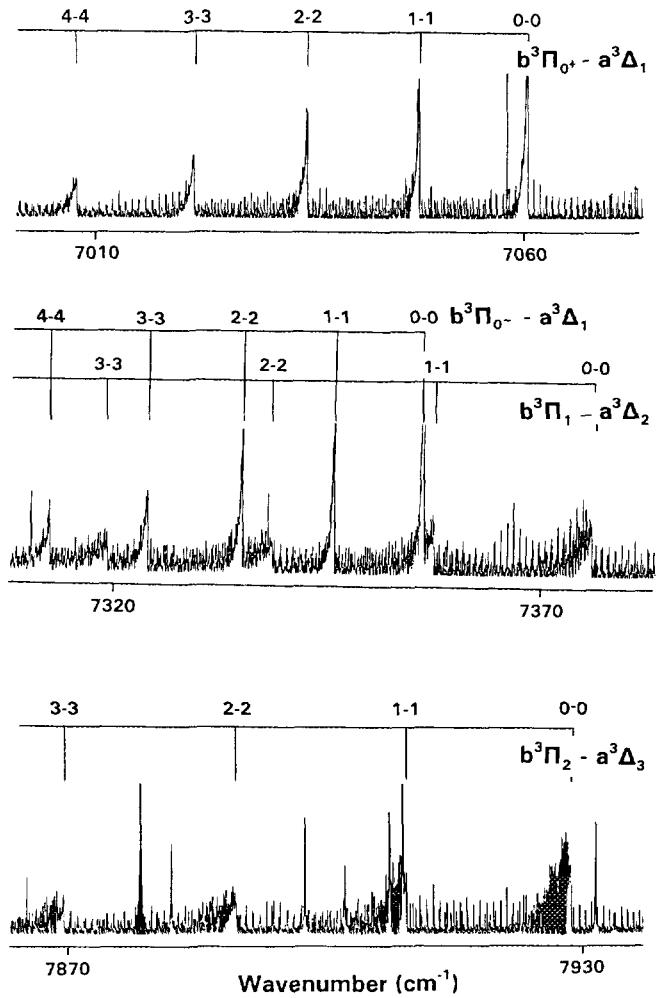

FIG. 2. A part of the compressed spectrum of the infrared system of HfO showing the sequence structure due to different subbands.

in these transitions do not have any observable Ω-doubling. It was pointed out by Edvinsson and Nylén (*40*) that these bands could be the subbands of a $^3\Phi$–$^3\Delta$ transition analogous to the $A^3\Phi$–$X^3\Delta$ transition of TiO (*41*) and the $b^3\Phi$–$a^3\Delta$ transition of ZrO (*42*).

In this paper we report the discovery of a new $^3\Pi$–$^3\Delta$ transition in the near infrared in the 6800–8000 cm^{-1} spectral region. These bands involve the same x_1, x_2, and x_3 lower states as observed by Edvinsson and Nylén in their $C - x_1$, $H - x_2$, and $J - x_3$ transitions (*40*). We have carried out a rotational analysis of the 0–0 and 1–1 bands and have determined the effective equilibrium constants in each state. The $a^3\Delta$ state is the lowest triplet state and the $b^3\Pi$ state is most probably the next excited triplet state of HfO. The $b^3\Pi$ and $a^3\Delta$ states of HfO are analogous to the $E^3\Pi$ and $X^3\Delta$ states of TiO (*43*). The corresponding $b'^3\Pi$–$a^3\Delta$ transition of ZrO has also been observed by laser photoluminescence of ZrO trapped in neon at 4 K (*44*) and in the gas phase (*15*).

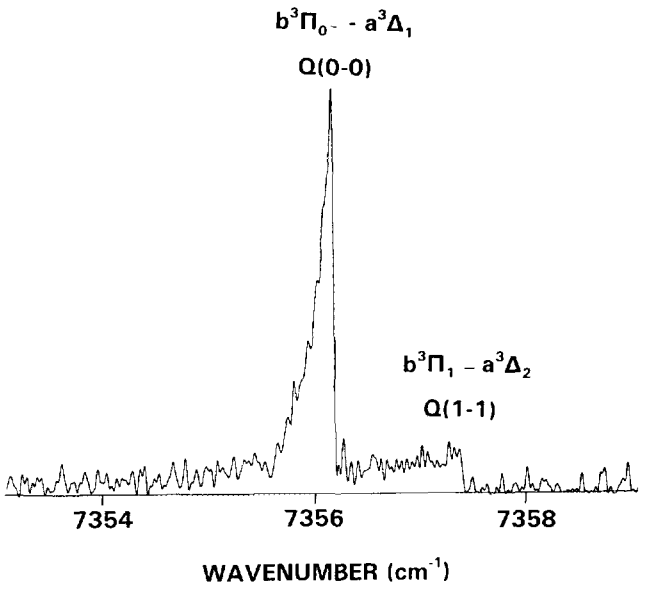

FIG. 3. A part of the spectrum showing the 0–0 band of the $b^3\Pi_0$–$a^3\Delta_1$ subband of HfO near the band origin. The intense and unresolved Q head appears due to the near equality of the molecular constants in the lower and upper excited states.

The present analysis allows a comparison of the electronic structure and bonding of TiO, ZrO, and HfO. For TiO and ZrO the leading configurations giving rise to the $^3\Delta$ and $^3\Pi$ states have been well established as $\pi^4\sigma\delta$ and $\pi^4\sigma\pi$ (*45–49*). There are no

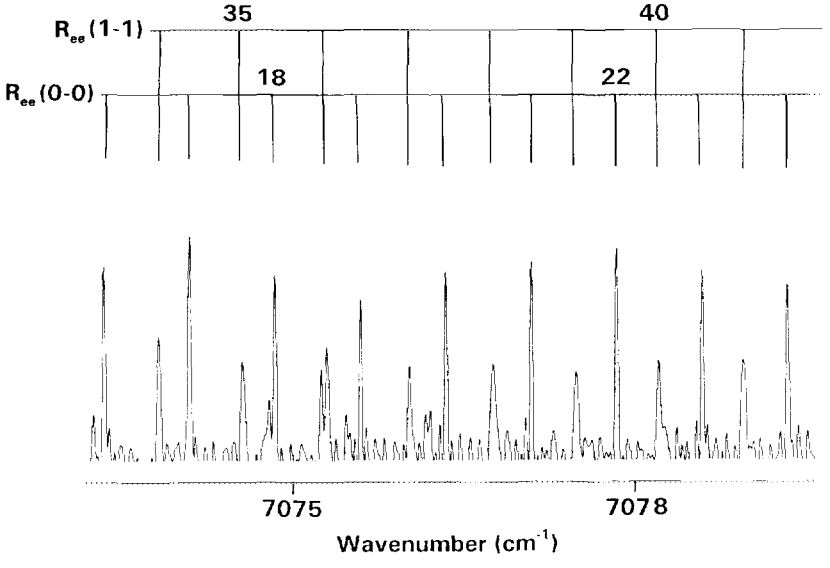

FIG. 4. A part of the spectrum of the $b^3\Pi_{0^-}$–$a^3\Delta_1$ subband of HfO showing a few R-branch lines of the 0–0 and 1–1 bands.

TABLE I

Observed Transition Wavenumbers (in cm^{-1}) of the 0–0 and 1–1 Bands of the $b^3\Pi_{0^+}$–$a^3\Delta_1$ Subband of HfO

	0-0 Band						1-1 Band					
J	Ree	O-C	Qef	O-C	Pee	O-C	Ree	O-C	Qef	O-C	Pee	O-C
3	7063.583	-0.009	-	-								
4	7064.347	0.002	-	-	7057.558	0.001	7051.579	0.001	-	-		
5	7065.098	0.002	-	-	7056.811	0.010	7052.319	-0.007	-	-	7044.067	-0.003
6	7065.851	0.003	-	-	7056.054	0.009	7053.068	-0.007	-	-	7043.308	-0.010
7	7066.601	0.002	-	-	7055.286	-0.002	7053.815	-0.008	-	-	7042.563	-0.002
8	7067.351	0.002	-	-	7054.525	-0.005	7054.563	-0.008	-	-	7041.805	-0.007
9	7068.100	-0.000	-	-	7053.768	-0.005	7055.312	-0.007	-	-	7041.048	-0.011
10	7068.852	0.003	-	-	7053.013	-0.002	7056.054	-0.012	-	-	7040.304	-0.002
11	7069.600	0.001	-	-	7052.253	-0.004	7056.811	-0.001	-	-	7039.554	0.002
12	7070.351	0.004	-	-	7051.496	-0.002	7057.558	-0.001	-	-	7038.800	0.002
13	7071.098	0.002	-	-	7050.737	-0.002	7058.307	0.002	-	-	7038.045	0.001
14	7071.843	-0.000	-	-	7049.974	-0.005	7059.063	0.014	-	-	7037.293	0.004
15	7072.591	0.001	-	-	7049.209	-0.010			-	-	7036.533	-0.002
16	7073.340	0.003	-	-	7048.450	-0.010			-	-	7035.781	0.002
17	7074.083	-0.001	-	-			7061.288	0.006	-	-	7035.027	0.003
18	7074.829	0.000	-	-	7046.935	-0.003	7062.023	-0.003	-	-		
19	7075.574	0.000	-	-	7046.178	0.001	7062.771	0.002	-	-	7033.500	-0.011
20	7076.319	0.001	-	-	7045.418	0.002	7063.513	0.002	-	-	7032.759	0.005
21	7077.062	0.000	-	-	7044.660	0.007	7064.255	0.002	-	-	7032.002	0.004
22	7077.804	-0.001	-	-	7043.899	0.007	7064.997	0.004	-	-	7031.243	0.003
23	7078.547	-0.001	-	-	7043.135	0.006	7065.738	0.005	-	-	7030.499	0.016
24	7079.290	0.000	-	-	7042.362	-0.004	7066.478	0.006	-	-	7029.729	0.004
25	7080.032	0.000	-	-	7041.617	0.013	7067.214	0.003	-	-	7028.973	0.007
26	7080.771	-0.001	-	-	7040.842	0.003	7067.953	0.003	-	-	7028.222	0.015
27	7081.510	-0.002	-	-	7040.079	0.003	7068.690	0.004	-	-	7027.460	0.012
28	7082.251	-0.001	-	-	7039.314	0.002	7069.425	0.001	-	-	7026.695	0.006
29	7082.989	-0.001	-	-	7038.550	0.002	7070.162	0.003	-	-	7025.937	0.009
30	7083.727	-0.002	-	-	7037.784	0.001	7070.890	-0.004	-	-	7025.174	0.007
31	7084.461	-0.005	-	-	7037.011	-0.007	7071.627	-0.001	-	-	7024.409	0.003
32	7085.202	-0.001	-	-	7036.261	0.008	7072.358	-0.003	-	-	7023.655	0.010
33	7085.934	-0.005	-	-	7035.477	-0.010	7073.093	0.000	-	-	7022.884	0.001
34	7086.671	-0.003	-	-			7073.817	-0.007	-	-	7022.121	0.001
35	7087.403	-0.006	-	-	7033.952	-0.003	7074.543	-0.011	-	-		
36	7088.143	0.000	-	-	7033.185	-0.004	7075.282	-0.002	-	-		
37	7088.869	-0.006	-	-	7032.422	0.001	7076.000	-0.012	-	-	7019.842	0.013
38	7089.592	-0.015	-	-	7031.659	0.005	7076.744	0.005	-	-	7019.064	0.001
39	7090.324	-0.015	-	-	7030.884	-0.002	7077.469	0.004	-	-	7018.288	-0.010
40	7091.066	-0.004	-	-	7030.114	-0.005	7078.175	-0.015	-	-	7017.519	-0.013
41	7091.798	-0.002	-	-	7029.351	0.001	7078.920	0.006	-	-	7016.760	-0.004
42	7092.535	0.006	-	-	7028.583	0.001	7079.633	-0.004	-	-	7015.996	-0.001
43	7093.267	0.011	-	-	7027.815	0.002	7080.352	-0.006	-	-	7015.224	-0.005
44	7093.994	0.010	-	-	7027.046	0.003	7081.075	-0.004	-	-	7014.463	0.003
45	7094.718	0.007	-	-	7026.275	0.001	7081.802	0.004	-	-	7013.686	-0.005

theoretical calculations available for HfO but the results obtained in this work are consistent with expectations based on the results of TiO and ZrO.

EXPERIMENTAL DETAILS

The HfO molecule was made in a hafnium hollow cathode lamp. The cathode was prepared by inserting a 1-mm-thick cylindrical foil of hafnium metal into a hole in a copper block. The foil was tightly pressed against the inner wall of the cathode to provide a close and uniform contact between the hafnium metal and the copper. The lamp was operated at 230 V and 248 mA with a continuous flow of 2.5 Torr of neon. A very small amount of oxygen (<3 mTorr) was required to excite the HfO bands while keeping the glow of the lamp steady. At higher pressures of O_2 the glow becomes unstable, even though the bands are more strongly developed. The emission from the hollow cathode was observed with the 1-m Fourier transform spectrometer associated with the McMath Solar Telescope of the National Solar Observatory.

TABLE I—*Continued*

	0-0 Band						1-1 Band					
J	Ree	O-C	Qef	O-C	Pee	O-C	Ree	O-C	Qef	O-C	Pee	O-C
46	7095.449	0.014	-	-	7025.494	-0.010	7082.517	0.001	-	-	7012.917	-0.004
47	7096.163	0.002	-	-	7024.734	-0.000	7083.233	0.001	-	-	7012.148	-0.002
48	7096.887	0.003	-	-	7023.966	0.002	7083.942	-0.006	-	-	7011.373	-0.005
49	7097.611	0.004	-	-	7023.190	-0.002	7084.658	-0.004	-	-	7010.607	0.001
50	7098.331	0.003	-	-	7022.423	0.001	7085.377	0.003	-	-	7009.828	-0.005
51	7099.056	0.006	-	-	7021.652	0.002	7086.099	0.014	-	-	7009.053	-0.006
52	7099.784	0.014	-	-	7020.881	0.003	7086.785	-0.010	-	-	7008.285	0.001
53	7100.483	-0.005	-	-	7020.108	0.002	7087.494	-0.010	-	-		
54	7101.208	0.001	-	-	7019.330	-0.004	7088.198	-0.012	-	-		
55	7101.923	-0.001	-	-	7018.563	0.003	7088.922	0.006	7047.065	-0.014	7005.946	-0.011
56	7102.642	0.003	-	-	7017.788	0.001	7089.618	-0.003	7047.035	-0.008	7005.182	0.002
57	7103.355	0.001	-	-	7017.015	0.001	7090.324	0.001	7047.015	0.008	7004.394	-0.007
58	7104.071	0.004	-	-	7016.242	0.003	7091.029	0.004	7046.977	0.008	7003.625	0.003
59	7104.796	0.015	-	-	7015.463	-0.002	7091.727	0.002	7046.931	0.001	7002.840	-0.003
60	7105.490	-0.002	-	-	7014.691	0.001	7092.427	0.004	7046.891	-0.000	7002.064	0.001
61	7106.207	0.005	-	-	7013.911	-0.005	7093.118	-0.002	7046.849	-0.001	7001.288	0.006
62	7106.904	-0.008	-	-	7013.141	0.001	7093.828	0.013	7046.807	-0.001		
63	7107.621	0.001	-	-	7012.361	-0.003	7094.539	0.029	7046.763	-0.004		
64	7108.320	-0.007	7059.580	0.011	7011.584	-0.004	7095.217	0.016	7046.717	-0.006		
65	7109.042	0.009	7059.539	0.007	7010.813	0.002	7095.900	0.007	7046.680	0.002		
66	7109.737	-0.001	7059.501	0.006	7010.027	-0.008	7096.605	0.023	7046.632	-0.000		
67	7110.447	0.005	7059.461	0.004	7009.269	0.011	7097.275	0.005	7046.588	0.002		
68	7111.137	-0.007	7059.415	-0.003	7008.472	-0.008			7046.540	0.002		
69	7111.853	0.008	7059.377	-0.002					7046.495	0.005		
70	7112.541	-0.003	7059.330	-0.008					7046.443	0.003		
71	7113.254	0.011	7059.289	-0.007					7046.393	0.003		
72	7113.947	0.007	7059.244	-0.010	7005.362	-0.003			7046.350	0.011		
73	7114.654	0.018	7059.203	-0.009	7004.591	0.005			7046.293	0.006		
74			7059.158	-0.009	7003.811	0.006			7046.241	0.006		
75			7059.118	-0.004	7003.039	0.014			7046.179	-0.002		
76			7059.066	-0.010	7002.234	-0.011			7046.128	0.000		
77			7059.029	-0.001	7001.463	-0.001			7046.071	-0.002		
78			7058.983	0.002	7000.690	0.008			7046.012	-0.005		
79			7058.932	-0.001	6999.916	0.016			7045.956	-0.006		
80			7058.880	-0.003	6999.114	-0.003			7045.897	-0.009		
81			7058.829	-0.003					7045.843	-0.007		
82			7058.780	-0.000								
83			7058.732	0.004	6996.766	-0.002						
84			7058.675	0.001	6995.993	0.009						
85			7058.620	0.001	6995.189	-0.010						
86			7058.568	0.004	6994.408	-0.007						

The spectra in the 2500–25 000 cm^{-1} wavenumber region were recorded in three parts. For the 2500–9200 cm^{-1} spectral region the spectrometer was operated with silicon filters and liquid-nitrogen-cooled InSb detectors and 10 scans were coadded in approximately 72 min of integration. For the 9000–21 000 cm^{-1} spectral region the spectrometer was operated with RG497 red pass filters and Si diode detectors and a total of 4 scans were coadded in 40 min of integration. For the 19 000–25 000 cm^{-1} region the spectrometer was operated with a $CuSO_4$ filter and Si diode detectors and 10 scans were coadded in 72 min of integration. For all three regions the spectrometer resolution was set at 0.02 cm^{-1}. The observed HfO infrared bands appear with a maximum signal-to-noise ratio of 20:1. The low J lines of this transition have a typical width of 0.026 cm^{-1}. At higher J, the lines slowly become broader due to isotope effects. Hafnium has six naturally occurring isotopes, ^{174}Hf(0.2%), ^{176}Hf(5.2%), ^{177}Hf(18.5%), ^{178}Hf(27.1%), ^{179}Hf(13.8%), and ^{180}Hf(35.2%). At higher J, the lines are partly split into two components due to the most abundant ^{178}HfO and ^{180}HfO isotopomers. The rotational constants have been determined using the line positions of the most abundant ^{180}HfO isotopomer.

TABLE II

Observed Transition Wavenumbers (in cm^{-1}) of the 0–0 and 1–1 Bands of the $b^3\Pi_0$–$a^3\Delta_1$ Subband of HfO

	0-0 Band						1-1 Band					
J	Rff	O-C	Qfe	O-C	Pff	O-C	Rff	O-C	Qfe	O-C	Pff	O-C
4			-	-	7353.169	0.001			-	-	7342.770	-0.005
5	7360.712	0.001	-	-	7352.420	0.007	7350.274	-0.008	-	-	7342.019	-0.005
6	7361.462	-0.001	-	-	7351.653	-0.004	7351.023	-0.009	-	-	7341.264	-0.008
7	7362.218	0.002	-	-	7350.913	0.012	7351.779	-0.003	-	-	7340.513	-0.008
8	7362.978	0.009	-	-	7350.143	-0.003	7352.522	-0.009	-	-	7339.767	-0.002
9	7363.733	0.011	-	-	7349.393	0.003	7353.278	-0.003	-	-	7339.018	-0.001
10	7364.473	0.000	-	-	7348.623	-0.011	7354.034	0.003	-	-		
11	7365.232	0.007	-	-	7347.884	0.007	7354.773	-0.006	-	-		
12	7365.984	0.008	-	-	7347.119	-0.002	7355.528	-0.001	-	-	7336.757	-0.006
13	7366.725	-0.003	-	-	7346.363	-0.002	7356.279	0.002	-	-	7336.012	0.001
14	7367.489	0.010	-	-	7345.604	-0.004	7357.028	0.003	-	-	7335.254	-0.005
15	7368.231	0.002	-	-	7344.850	-0.001	7357.778	0.004	-	-		
16	7368.979	-0.001	-	-	7344.087	-0.008	7358.529	0.007	-	-	7333.757	0.002
17	7369.730	0.000	-	-	7343.333	-0.005	7359.274	0.005	-	-	7332.995	-0.008
18	7370.480	0.001	-	-	7342.565	-0.016	7360.026	0.010	-	-	7332.251	0.001
19	7371.233	0.004	-	-	7341.821	-0.002	7360.770	0.007	-	-	7331.504	0.006
20	7371.985	0.008	-	-	7341.051	-0.015	7361.515	0.006	-	-	7330.739	-0.006
21	7372.731	0.005	-	-	7340.298	-0.011	7362.261	0.005	-	-	7330.000	0.008
22	7373.478	0.004	-	-	7339.542	-0.008	7363.007	0.007	-	-	7329.254	0.014
23	7374.215	-0.007	-	-	7338.794	0.001	7363.760	0.014	-	-	7328.486	-0.000
24	7374.961	-0.008	-	-	7338.036	0.001	7364.498	0.008	-	-	7327.732	-0.001
25	7375.720	0.004	-	-			7365.232	-0.002	-	-	7326.983	0.004
26	7376.463	0.000	-	-	7336.525	0.005	7365.984	0.006	-	-	7326.233	0.008
27	7377.208	-0.002	-	-	7335.751	-0.011	7366.726	0.005	-	-	7325.478	0.007
28	7377.953	-0.002	-	-			7367.465	0.001	-	-	7324.719	0.001
29	7378.702	0.002	-	-	7334.241	-0.004	7368.193	-0.013	-	-		
30	7379.445	-0.001	-	-	7333.501	0.014	7368.940	-0.007	-	-		
31	7380.191	0.001	-	-	7332.730	0.002	7369.681	-0.006	-	-	7322.466	0.013
32	7380.930	-0.004	-	-	7331.980	0.010	7370.428	0.001	-	-	7321.706	0.008
33	7381.673	-0.004	-	-	7331.211	0.001	7371.168	0.001	-	-	7320.948	0.006
34	7382.412	-0.008	-	-	7330.450	-0.002	7371.898	-0.007	-	-	7320.194	0.008
35	7383.151	-0.011	-	-	7329.699	0.006	7372.635	-0.008	-	-	7319.427	-0.003
36	7383.884	-0.020	-	-	7328.934	0.000	7373.367	-0.013	-	-	7318.674	0.000
37	7384.636	-0.009	-	-	7328.168	-0.007	7374.116	0.000	-	-	7317.929	0.012
38	7385.378	-0.008	-	-	7327.413	-0.002	7374.836	-0.015	-	-	7317.168	0.008
39	7386.117	-0.009	-	-	7326.659	0.003	7375.595	0.009	-	-	7316.403	0.001
40	7386.850	-0.015	unresolved		7325.898	0.002	7376.330	0.010	unresolved		7315.633	-0.010
41	7387.596	-0.008	Q-head at		7325.138	0.000	7377.069	0.016	Q-head at		7314.876	-0.009
42	7388.333	-0.009	7356.165 cm		7324.375	-0.002	7377.791	0.007	7345.762 cm		7314.124	-0.002
43	7389.064	-0.017	-	-	7323.618	-0.000	7378.518	0.003	-	-	7313.370	0.003
44	7389.802	-0.015	-	-	7322.860	0.002	7379.240	-0.004	-	-		
45	7390.556	0.002	-	-	7322.102	0.004	7379.972	-0.001	-	-	7311.844	-0.003

In addition to HfO bands there are many Hf and Ne atomic lines present in our spectra. The spectra were calibrated using the measurements of the Ne atomic lines made by Palmer and Engleman (*50*). The absolute accuracy of the wavenumber scale is expected to be better than ± 0.002 cm^{-1}. However, overlapping lines and unresolved isotopic splittings limited the precision of the observed HfO line positions to ± 0.003 cm^{-1}.

OBSERVATION AND ANALYSIS

The rotational lines were measured using a data reduction program called PC-DECOMP developed by J. Brault of the National Solar Observatory at Kitt Peak. The line centers were determined by fitting the line profiles to Voigt lineshape functions. The assignment of the HfO lines was facilitated by an interactive color Loomis–Wood program which is very useful for the analysis of weak and complex spectra.

In the visible region the spectra of HfO are basically the same as observed by Edvinsson and Nylén (*40*). But in the infrared a new system of HfO has been identified.

TABLE II—*Continued*

	0-0 Band						1-1 Band					
J	Rff	O-C	Qfe	O-C	Pff	O-C	Rff	O-C	Qfe	O-C	Pff	O-C
46	7391.278	-0.012	-	-	7321.334	-0.004	7380.697	-0.005	-	-	7311.094	0.008
47	7392.035	0.010	-	-	7320.578	0.000	7381.428	0.000	-	-	7310.329	0.004
48	7392.762	0.003	-	-	7319.815	-0.002	7382.152	-0.001	-	-	7309.560	-0.004
49	7393.499	0.006	-	-			7382.876	-0.002	-	-	7308.785	-0.016
50	7394.227	0.002	-	-	7318.301	0.005	7383.601	-0.000	-	-	7308.030	-0.009
51	7394.964	0.007	-	-	7317.541	0.005	7384.323	-0.001	-	-	7307.259	-0.017
52	7395.690	0.001	-	-	7316.764	-0.011	7385.037	-0.008	-	-	7306.505	-0.007
53	7396.423	0.003	-	-	7316.025	0.011	7385.774	0.009	-	-	7305.749	0.000
54	7397.157	0.008	-	-	7315.261	0.008	7386.482	-0.002	-	-	7304.981	-0.003
55	7397.868	-0.010	-	-	7314.497	0.006	7387.196	-0.005	-	-	7304.212	-0.006
56	7398.616	0.010	-	-	7313.724	-0.006	7387.909	-0.009	-	-	7303.451	-0.002
57	7399.330	-0.004	-	-	7312.973	0.005	7388.633	0.000	-	-		
58	7400.059	-0.002	-	-			7389.342	-0.005	-	-		
59	7400.777	-0.010	-	-	7311.433	-0.012	7390.060	0.000	-	-		
60	7401.506	-0.006	-	-	7310.685	0.001			-	-		
61	7402.246	0.011	-	-	7309.929	0.007					7299.621	0.004
62	7402.967	0.008	-	-	7309.157	-0.003					7298.843	-0.005
63	7403.669	-0.011	-	-	7308.394	-0.004					7298.082	0.003
64	7404.400	-0.002	-	-	7307.636	0.001					7297.307	-0.003
65	7405.126	0.004	-	-	7306.872	-0.001					7296.535	-0.004
66	7405.843	0.002	-	-	7306.112	0.003					7295.780	0.010
67	7406.562	0.002	-	-	7305.350	0.004					7295.008	0.009
68	7407.273	-0.005	-	-	7304.585	0.001					7294.232	0.004
69	7407.998	0.005	-	-	7303.825	0.004						
70	7408.724	0.015	-	-	7303.066	0.010						
71	7409.418	-0.005	-	-	7302.303	0.010						
72	7410.127	-0.010	-	-								
73	7410.849	0.000	-	-								
74	7411.567	0.007	-	-								
75	7412.275	0.004	-	-								
76	7412.975	-0.005	-	-								
77	7413.665	-0.022	-	-								
78	7414.391	-0.003	-	-								
79			-	-								
80	7415.799	-0.005	-	-								
81	7416.500	-0.008	-	-								
82			-	-								
83	7417.913	0.002	-	-								
84	7418.638	0.028	-	-								

The new bands of HfO are located in the 6900–8000 cm^{-1} spectral region and have been assigned to a $^3\Pi$–$^3\Delta$ transition. A schematic energy level diagram of the observed subbands of this transition is presented in Fig. 1, where the band origin of the 0–0 band in each subband is marked. A part of the compressed spectrum of the infrared bands is presented in Fig. 2, showing the sequence structure present in each subband. The spectrum consists of three well separated groups of bands. The bands in the 6900–7100 cm^{-1} region consist of a single sequence of bands with head-to-head separations of about 12 cm^{-1}. These bands have been identified as due to the $^3\Pi_{0^+}$–$^3\Delta_1$ subband. The 7200–7400 cm^{-1} spectral region consists of two sequences of bands, one with successive head-to-head separations of about 11 cm^{-1} and the other with separations of about 19 cm^{-1}. After rotational analysis, the first sequence has been identified as the $^3\Pi_{0^-}$–$^3\Delta_1$ transition and the other sequence has been identified as the $^3\Pi_1$–$^3\Delta_2$ subband. The third group consists of a single sequence of bands with successive head-to-head separations of about 20 cm^{-1}, which have been identified as the $^3\Pi_2$–$^3\Delta_3$ subband.

The bands in each subband region consist of many diagonal $\Delta v = 0$ bands (up to $v' = v'' = 11$). No off-diagonal bands with $\Delta v \neq 0$ were observed in our spectra because of the near equality of the vibrational and rotational constants in the lower and excited

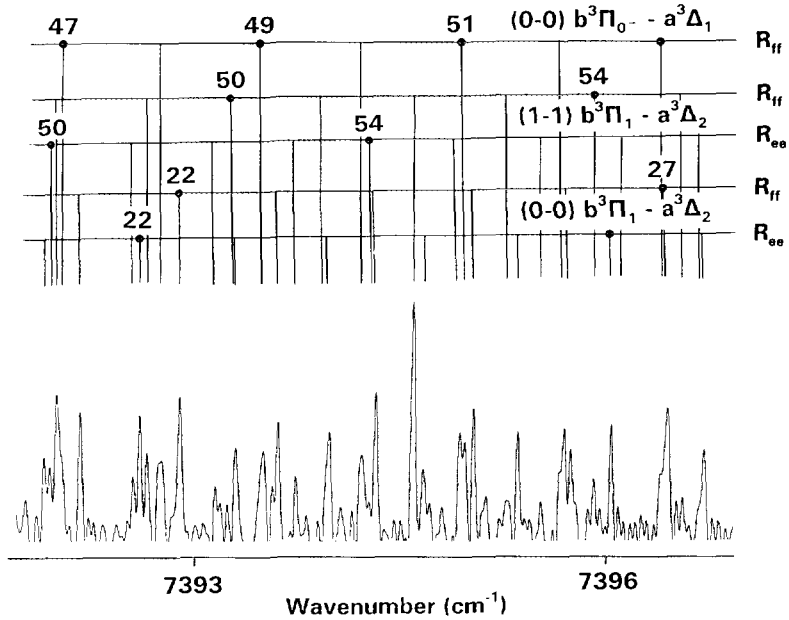

FIG. 5. A part of the spectrum of the $b^3\Pi_1$–$a^3\Delta_2$ Subband of HfO showing a few R-branch lines of the 0–0 and 1–1 bands. The overlapping high-J R-branch lines of the 0–0 band of the $b^3\Pi_0$–$a^3\Delta_1$ subband have also been marked.

states. This near equality of the rotational constants also means that the Q-branch lines are resolved only at high J values in most of the bands. In fact, in the $^3\Pi_{0^-}$–$^3\Delta_1$ subband all of the Q-branch lines are piled up within 0.6 cm^{-1}, resulting in a broad and intense Q head, slightly degraded toward lower wavenumbers (Fig. 3). In the $^3\Pi_{0^+}$–$^3\Delta_1$ subband the Q-branch lines could be resolved after $Q(64)$ in the 0–0 band. In the $^3\Pi_1$–$^3\Delta_2$ and $^3\Pi_2$–$^3\Delta_3$ subbands the Q-branch lines could be picked out for relatively low J values. In most of the observed bands the intensities of the P and R branches are similar and the Q branch is about twice as strong as the P and R branches.

A part of the spectrum of the 0–0 band of the $^3\Pi_{0^+}$–$^3\Delta_1$ subband is presented in Fig. 4. The structure of this band consists of single P, Q, and R branches. The analysis of $^3\Pi_{0^-}$–$^3\Delta_1$ and $^3\Pi_{0^+}$–$^3\Delta_1$ subbands with a common lower state was accomplished by comparing the lower state combination differences. Because of the large separation between the 0^+ and 0^- components (295.61 cm^{-1}), both of these components were treated as independent states. The observed rotational lines were fitted to the usual Hund's case (c) energy level expression:

$$F_v(J) = T_v + B_vJ(J+1) - D_v[J(J+1)]^2 + H_v[J(J+1)]^3 \pm (1/2)\{q(J(J+1) + q_D[J(J+1)]^2 + q_H[J(J+1)]^3\}. \quad (1)$$

The rotational structures of the 0–0 and 1–1 bands of both of these subbands were measured and the line positions were used to determine the rotational constants in the lower and the excited states. The line positions for the 0–0 and 1–1 bands of the $^3\Pi_{0^+}$–$^3\Delta_1$ and $^3\Pi_{0^-}$–$^3\Delta_1$ subbands are provided in Tables I and II. The rotational constants for the 0^+ and 0^- components of the $b^3\Pi$ state are found to be similar although these two levels are separated by 295.61 and 297.95 cm^{-1} in the $v = 0$ and

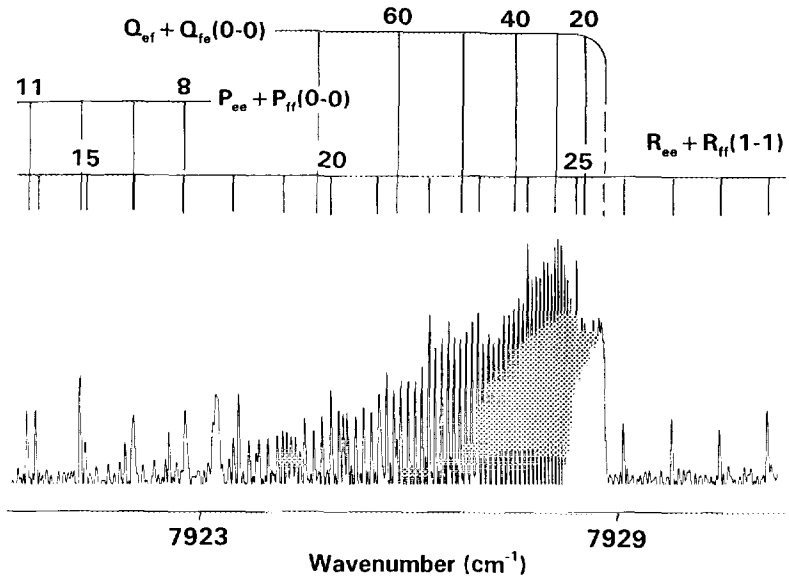

FIG. 6. A part of the spectrum of the $b^3\Pi_2$-$a^3\Delta_3$ subband of HfO near the Q head of the 0–0 band origin.

1 vibrational levels. The rotational analysis of the 2–2 and higher vibrational bands was not attempted due to the complexity resulting from overlapping bands as well as the increasing broadening arising from the isotope effect.

A part of the 0–0 band of the $^3\Pi_1$-$^3\Delta_2$ subband is provided in Fig. 5. This band also consists of P, Q, and R branches with each line doubled due to Ω-doubling in the excited $^3\Pi_1$ spin component. The present analysis shows that there is no Ω-doubling in the lower $a^3\Delta_2$ state. In the excited $^3\Pi_1$ state, in addition to B_v and D_v, the Ω-doubling parameters q and q_D were also required in order to obtain a satisfactory fit. The rotational analysis of the 0–0 and 1–1 bands of this transition was obtained and the observed transition wavenumbers were fitted to the Hund's case (c) energy expression, Eq. (1). The observed transition wavenumbers of the 0–0 and 1–1 bands of this subband are provided in Table III.

On the high wavenumber side of the $^3\Pi_1$-$^3\Delta_2$ subband, a band with a Q head at 7929.5 cm^{-1} has been identified as the 0–0 band of the $^3\Pi_2$-$^3\Delta_3$ subband. A part of the rotational structure of this band is presented in Fig. 6. The rotational structure of this subband consists of single P, Q, and R branches. As in the case of $^3\Pi_0$-$^3\Delta_1$ and $^3\Pi_1$-$^3\Delta_2$ subbands, the high J rotational lines of this subband are also broadened and are partially split into two components due to the isotope effect. The analysis of this subband indicates that there is no Ω-doubling in either the $^3\Pi_2$ or the $^3\Delta_3$ spin components. The rotational structure of the 0–0 and 1–1 bands of this subband was analyzed in a similar manner to that described for the other two subbands. The line positions of the 0–0 and 1–1 bands of this subband are provided in Table IV.

The signs of the Ω-doubling constants were determined by assuming that a $^3\Sigma^-$ state lies above the $b^3\Pi$ state, as in ZrO. Assuming a pure precession interaction (*51*, *52*) means that the $^3\Pi_{0^-}$ spin component lies above $^3\Pi_{0^+}$ and that the f-parity level lies above the e-parity level in the $^3\Pi_1$ spin component. For the Hund's case (c) energy level expression (Eq. 1) this means that q is negative for the $b^3\Pi_1$ spin component.

TABLE III

Observed Transition Wavenumbers (in cm^{-1}) of the 0–0 and 1–1 Bands of the $b^3\Pi_1$–$a^3\Delta_2$ Subband of HfO

	0-0 Band											
J	Rff	O-C	Qfe	O-C	Pff	O-C	Ree	O-C	Qef	O-C	Pee	O-C
4	7379.715	-0.001	-	-	7372.929	0.001	-	-	-	-	-	-
5	7380.461	-0.001	-	-	7372.167	0.002	-	-	-	-	-	-
6	7381.206	-0.001	-	-	7371.412	0.011	-	-	-	-	-	-
7			-	-	7370.620	-0.016	-	-	-	-	7370.616	0.002
8	7382.709	0.019	-	-	7369.860	-0.009	-	-	-	-	7369.824	-0.016
9	7383.440	0.011	-	-			7383.390	0.017	-	-	7369.069	0.007
10	7384.177	0.010	-	-	7368.326	-0.004	7384.114	0.015	-	-	7368.287	0.004
11	7384.911	0.008	-	-	7367.560	0.002	7384.826	0.004	-	-	7367.489	-0.012
12	7385.641	0.004	-	-	7366.780	-0.004	7385.548	0.005	-	-	7366.726	0.010
13	7386.373	0.004	-	-	7366.014	0.005	7386.262	0.001	7375.720	0.002	7365.928	-0.000
14	7387.106	0.006	-	-	7365.232	-0.001	7386.983	0.006	7375.683	0.001	7365.130	-0.008
15	7387.828	-0.002	-	-	7364.442	-0.013	7387.669	-0.020	7375.636	-0.006	7364.341	-0.006
16	7388.556	-0.002	-	-	7363.665	-0.011	7388.404	0.004	7375.595	-0.004	7363.548	-0.004
17	7389.293	0.010	-	-	7362.889	-0.006	7389.109	0.002	7375.553	-0.002	7362.757	0.003
18	7390.011	0.003	-	-	7362.106	-0.006	7389.824	0.012	7375.504	-0.002	7361.952	-0.003
19	7390.733	0.003	-	-	7361.328	-0.001	7390.524	0.011	7375.460	0.003	7361.146	-0.006
20	7391.445	-0.007	7375.636	0.015	7360.522	-0.022	7391.207	-0.005	7375.391	-0.013	7360.347	-0.000
21	7392.169	-0.002	7375.595	0.007	7359.758	0.000	7391.906	-0.003	7375.345	-0.004	7359.542	0.001
22	7392.889	0.001	7375.553	0.000	7358.964	-0.006	7392.600	-0.003	7375.295	0.004	7358.708	-0.023
23	7393.602	-0.002	7375.504	-0.011	7358.191	0.010	7393.298	0.003	7375.212	-0.019	7357.902	-0.016
24	7394.317	-0.002	7375.460	-0.018	7357.380	-0.010	7393.976	-0.007	7375.161	-0.007	7357.112	0.008
25	7395.030	-0.001	7375.431	-0.007	7356.586	-0.011	7394.664	-0.004	7375.107	0.005	7356.279	-0.009
26	7395.738	-0.005	7375.391	-0.006			7395.353	0.001	7375.058	0.023	7355.466	-0.002
27	7396.445	-0.006	7375.345	-0.010	7355.017	0.008	7396.029	-0.004	7374.961	-0.003	7354.630	-0.017
28	7397.157	-0.002	7375.295	-0.016	7354.215	0.002	7396.704	-0.007	7374.891	-0.001	7353.823	-0.011
29	7397.868	0.003	7375.257	-0.008	7353.418	0.001	7397.383	-0.003	7374.836	0.020	7353.001	0.004
30	7398.570	0.000	7375.212	-0.006	7352.620	0.002	7398.057	-0.001	7374.725	-0.014	7352.182	0.013
31	7399.270	-0.002	7375.161	-0.008	7351.809	-0.009	7398.728	-0.000	7374.657	-0.001	7351.344	0.006
32	7399.972	-0.001	7375.107	-0.012	7351.023	0.007	7399.393	-0.003	7374.583	0.007	7350.513	0.008
33	7400.673	0.000	7375.058	-0.010	7350.222	0.008	7400.059	-0.001	7374.473	-0.018		
34	7401.373	0.003	7375.014	-0.001	7349.409	-0.002	7400.728	0.006	7374.399	-0.004	7348.836	0.003
35	7402.061	-0.006	7374.961	0.000	7348.623	0.017	7401.373	-0.008	7374.317	0.004	7347.997	0.004
36	7402.757	-0.005	7374.891	-0.015	7347.799	-0.001	7402.023	-0.015	7374.215	-0.005	7347.156	0.004
37	7403.459	0.004	7374.836	-0.012	7347.000	0.006	7402.693	0.000	7374.116	-0.009	7346.312	0.004
38	7404.146	-0.000	7374.786	-0.004	7346.189	0.004	7403.346	0.002	7374.032	0.003		
39	7404.836	0.001	7374.725	-0.006	7345.380	0.005	7403.994	0.002	7373.923	-0.006	7344.608	-0.005
40	7405.525	0.002	7374.657	-0.012	7344.573	0.009	7404.647	0.009	7373.818	-0.008	7343.764	0.002
41	7406.208	-0.001	7374.614	0.007	7343.764	0.012	7405.289	0.007	7373.731	0.010	7342.915	0.005
42	7406.903	0.009	7374.537	-0.005			7405.929	0.007	7373.614	-0.001	7342.072	0.017
43	7407.579	0.002	7374.473	-0.004	7342.135	0.010	7406.562	0.002	7373.504	-0.001	7341.212	0.014
44	7408.264	0.007	7374.399	-0.011	7341.317	0.007	7407.198	0.002	7373.393	-0.001	-	-
45	7408.945	0.008	7374.317	-0.024	7340.513	0.020	7407.836	0.007	7373.301	0.021	-	-
46	7409.622	0.008	7374.270	-0.001	7339.680	0.004	7408.470	0.011	7373.169	0.006	-	-
47	7410.292	0.002	7374.215	0.016	7338.863	0.007	7409.089	0.004	7373.035	-0.009	-	-
48	7410.961	-0.003	7374.116	-0.030			7409.716	0.006	7372.929	0.007	-	-
49	7411.638	0.002	7374.032	-0.021			7410.326	-0.005	7372.795	-0.003	-	-
50	7412.314	0.008	7373.975	-0.001	7336.402	0.010	7410.961	0.010	7372.661	-0.010	-	-
51	7412.975	-0.000	7373.888	-0.011	7335.577	0.008	7411.567	0.001	7372.542	-0.000	-	-
52	7413.641	-0.001	7373.838	-0.001			7412.178	-0.002	7372.412	0.001	-	-
53	7414.306	-0.000	7373.731	-0.007	7333.927	0.010	7412.789	-0.001	7372.273	-0.003	-	-
54	7414.979	0.010	7373.652	-0.005	7333.117	0.028	7413.398	0.001	7372.121	-0.019	-	-
55	7415.626	-0.004	7373.567	-0.005	7332.251	-0.009	7413.994	-0.008	7371.985	-0.015	-	-
56	7416.291	0.002	7373.478	-0.009	7331.428	-0.002	7414.581	-0.022	7371.851	-0.007	-	-
57	7416.948	0.003	7373.393	-0.006			7415.197	-0.004	7371.709	-0.005	-	-
58	7417.596	-0.003	7373.301	-0.009	7329.782	0.017	7415.799	0.003	7371.545	-0.022	-	-
59	7418.253	0.002	7373.224	0.005	7328.934	0.004	7416.390	0.001	7371.412	-0.004	-	-
60	7418.900	-0.002	7373.132	0.006			7416.969	-0.008	7371.273	0.010	-	-
61	7419.565	0.016	7373.035	0.003	7327.256	0.000	7417.564	0.000	7371.100	-0.008	-	-
62			7372.929	-0.006			7418.140	-0.006	7370.931	-0.018	-	-
63			7372.836	0.000			7418.735	0.010	7370.778	-0.009	-	-
64			7372.731	-0.003					7370.620	-0.002	-	-
65			7372.635	0.004					7370.480	0.026	-	-
66									7370.283	0.000	-	-
67									7370.118	0.009	-	-
68									7369.936	0.004	-	-
69									7369.770	0.020	-	-

TABLE III—*Continued*

	1-1 Band											
J	Rff	O-C	Qfe	O-C	Pff	O-C	Ree	O-C	Qef	O-C	Pee	O-C
4	-	-	-	-	-	-	-	-			7354.390	-0.002
5	-	-	-	-	-	-	-	-	-	-	7353.625	-0.003
6	-	-	-	-	-	-	-	-	-	-	7352.872	0.010
7	-	-	-	-	-	-	-	-	-	-	7352.088	-0.005
8	-	-	-	-	-	-	7364.056	-0.005	-	-	7351.344	0.023
9	-	-	-	-	-	-	7364.762	-0.023	-	-	7350.553	0.006
10	-	-	-	-	-	-	7365.506	0.001	-	-	7349.784	0.015
11	-	-	-	-	-	-	7366.220	-0.004	-	-	7349.015	0.026
12	-	-	-	-	7348.265	-0.010	7366.938	-0.000	-	-	7348.214	0.007
13	7367.755	-0.004	-	-	7347.491	-0.010	7367.658	0.008	-	-	7347.408	-0.013
14	7368.479	-0.004	-	-	7346.719	-0.007			-	-	7346.634	0.002
15	7369.209	0.002	-	-			7369.069	0.003	7357.080	0.000		
16	7369.936	0.008	-	-			7369.770	0.001	7357.028	-0.006		
17	7370.648	0.001	-	-	7344.390	-0.000	7370.480	0.010	7356.976	-0.010	7344.260	0.010
18	7371.365	0.001	-	-	7343.596	-0.013	7371.168	0.000	7356.930	-0.006	7343.461	0.010
19	7372.078	-0.001	-	-	7342.817	-0.009	7371.851	-0.011	7356.880	-0.002	7342.645	-0.004
20	7372.795	0.002	-	-	7342.019	-0.022	7372.542	-0.012	7356.827	0.002		
21	7373.504	-0.000	-	-	7341.263	0.009	7373.224	-0.019	7356.781	0.014	7341.051	0.013
22	7374.215	0.001	7356.976	0.011	7340.444	-0.021	7373.923	-0.007	7356.731	0.027	7340.231	0.004
23			7356.930	0.005	7339.678	0.002	7374.614	0.001	7356.635	-0.005	7339.444	0.029
24	7375.636	0.008	7356.880	-0.002	7338.867	-0.017	7375.295	0.002	7356.586	0.014		
25	7376.330	-0.002	7356.827	-0.010	7338.085	-0.006			7356.516	0.014		
26	7377.033	-0.001	7356.781	-0.010			7376.647	0.002	7356.415	-0.015	7336.967	0.006
27	7377.744	0.010	7356.731	-0.012	7336.495	-0.004	7377.323	0.007	7356.348	-0.006	7336.147	0.009
28	7378.425	-0.007	7356.691	-0.003	7335.712	0.010	7377.990	0.005	7356.279	0.004	7335.314	0.002
29	7379.133	0.004	7356.635	-0.007			7378.649	-0.001	-	-		
30	7379.824	0.001	7356.586	-0.002	7334.104	0.002	7379.305	-0.008	-	-	7333.667	0.013
31	7380.519	0.003			7333.294	-0.005	7379.972	-0.001	-	-	7332.823	0.003
32	7381.202	-0.005	7356.474	-0.003	7332.500	0.005	7380.625	-0.005	-	-	7331.980	-0.005
33	7381.899	0.004	7356.415	-0.004	7331.694	0.005	7381.282	-0.001	-	-	7331.147	0.001
34	7382.585	0.003	7356.348	-0.011	7330.883	0.001	7381.934	-0.000	-	-	7330.306	0.001
35	7383.267	-0.000	7356.279	-0.018	7330.077	0.004	7382.585	0.003	-	-	7329.461	-0.001
36	7383.949	-0.001	7356.232	-0.001	7329.254	-0.010	7383.229	0.001	-	-	7328.612	-0.004
37	7384.636	0.005	-	-	7328.461	0.009	7383.884	0.014	-	-		
38	7385.308	-0.002	-	-	7327.637	-0.001	7384.517	0.007	-	-	7326.914	-0.003
39	7385.991	0.004	-	-	7326.819	-0.005	7385.140	-0.006	-	-	7326.068	0.005
40	7386.667	0.006	-	-	7326.015	0.007	7385.774	-0.005	7355.121	0.000	7325.191	-0.016
41	7387.334	-0.001	-	-	7325.191	0.001	7386.429	0.020	7355.017	0.010	7324.346	-0.003
42	7388.001	-0.005	-	-	7324.375	0.004	7387.036	-0.001	7354.878	-0.012		
43	7388.674	-0.001	-	-			7387.669	0.008	7354.773	0.002	7322.631	0.006
44	7389.342	-0.001	-	-	7322.728	-0.000			7354.661	0.012	7321.759	0.000
45	7390.011	0.004	-	-			7388.902	0.001	7354.526	0.002	7320.912	0.021
46	7390.667	-0.004	-	-	7321.078	-0.002	7389.518	0.002	7354.390	-0.007	7320.029	0.009
47	7391.336	0.005	-	-	7320.260	0.007	7390.130	0.001	7354.258	-0.009		
48	7391.999	0.009	-	-			7390.733	-0.005	7354.128	-0.006		
49	7392.651	0.004	-	-	7318.602	0.006	7391.336	-0.008	7353.993	-0.005	7317.408	0.015
50	7393.298	-0.004	7355.157	-0.005	7317.762	-0.003	7391.946	-0.001	7353.851	-0.008	7316.506	-0.006
51	7393.949	-0.006	7355.077	0.005	7316.928	-0.005	7392.553	0.005	7353.699	-0.020	7315.633	0.004
52	7394.588	-0.017	7354.979	-0.001	7316.088	-0.011	7393.147	0.002	7353.561	-0.013	7314.742	-0.003
53	7395.263	0.009	7354.878	-0.009	7315.261	-0.003	7393.732	-0.007	7353.418	-0.010	7313.865	0.009
54	7395.904	0.005	7354.773	-0.019	7314.424	-0.003	7394.317	-0.013	7353.278	-0.000	7312.973	0.007
55	7396.549	0.006	7354.693	-0.002	7313.582	-0.005	7394.929	0.011	7353.112	-0.014		
56			7354.586	-0.010			7395.518	0.016	7352.964	-0.007	7311.181	0.003
57	7397.844	0.019	7354.483	-0.012			7396.086	0.002	7352.820	0.007	7310.295	0.015
58	7398.476	0.014	7354.390	-0.003			7396.664	0.002	7352.649	-0.002	7309.382	0.002
59			7354.280	-0.008			7397.241	0.004	7352.475	-0.013	7308.485	0.007
60	7399.735	0.004	7354.177	-0.004			7397.796	-0.013	7352.317	-0.004		
61	7400.363	0.002	7354.080	0.007					7352.136	-0.016	7306.656	-0.008
62	7401.006	0.017	7353.949	-0.013					7351.973	-0.006	7305.749	-0.005
63	7401.617	0.003	7353.851	0.002			7399.487	-0.018	7351.809	0.005	7304.847	0.007
64	7402.246	0.009	7353.729	-0.006			7400.059	-0.004			7303.930	0.005
65	7402.853	-0.005	7353.625	0.007			7400.617	-0.001			7303.017	0.010
66	7403.472	-0.004	7353.476	-0.024			7401.169	-0.000				
67	7404.073	-0.019	7353.378	-0.000			7401.695	-0.023				
68	7404.708	0.004	7353.278	0.022			7402.246	-0.036				
69			7353.136	0.006			7402.819	0.015				
70			7353.001	-0.001			7403.346	0.005				
71			7352.872	0.000			7403.878	0.003				
72			7352.726	-0.014			7404.400	-0.005				
73			7352.620	0.015								
74			7352.475	0.008								
75			7352.317	-0.010								
76			7352.182	-0.003								

TABLE IV

Observed Transition Wavenumbers (in cm^{-1}) of the 0–0 and 1–1 Bands of the $b^3\Pi_2$–$a^3\Delta_3$ Subband of HfO

	0-0 Band						1-1 Band					
J	Ree+Rff	O-C	Qef+Qfe	O-C	Pee+Pff	O-C	Ree+Rff	O-C	Qef+Qfe	O-C	Pee+Pff	O-C
5					7925.070	-0.006	7913.984	-0.004			7905.720	0.001
6	7934.131	-0.003	-	-	7924.309	-0.001	7914.742	0.013	-	-	7904.953	-0.004
7	7934.883	0.005	-	-	7923.543	-0.001	7915.477	0.009	-	-	7904.187	-0.005
8	7935.621	0.000	-	-	7922.763	-0.013	7916.206	0.002	-	-	7903.422	-0.003
9	7936.365	0.004	-	-	7921.993	-0.013	7916.942	0.002	-	-	7902.644	-0.014
10	7937.100	-0.001	-	-	7921.235	0.001	7917.676	0.004	-	-	7901.885	-0.002
11	7937.830	-0.008	-	-	7920.459	-0.002	7918.406	0.002	-	-	7901.105	-0.011
12	7938.576	0.002	-	-	7919.684	-0.003	7919.130	-0.002	-	-	7900.344	0.001
13	7939.310	0.002	-	-	7918.910	-0.001	7919.859	-0.001	-	-	7899.576	0.008
14	7940.047	0.007	-	-	7918.130	-0.003	7920.590	0.005	-	-	7898.804	0.013
15	7940.772	0.001	-	-	7917.354	0.000	7921.307	-0.002	-	-	7898.014	0.002
16	7941.503	0.003	-	-	7916.569	-0.004	7922.022	-0.008	-	-	7897.237	0.006
17			-	-	7915.788	-0.003	7922.763	0.014	-	-	7896.456	0.007
18	7942.956	0.003	-	-	7915.002	-0.005	7923.465	-0.001	-	-	7895.671	0.006
19	7943.686	0.010	-	-	7914.217	-0.004	7924.184	0.002	7909.159	0.003	7894.888	0.009
20	7944.402	0.004	-	-	7913.433	-0.002	7924.891	-0.004	7909.116	-0.002	7894.094	0.002
21	7945.122	0.004	-	-	7912.636	-0.010	7925.608	0.002	7909.071	-0.009	7893.292	-0.011
22	7945.839	0.003	7928.478	0.008	7911.854	-0.003	7926.308	-0.008	7909.030	-0.009	7892.517	0.006
23	7946.557	0.005	7928.435	0.003	7911.059	-0.006	7927.015	-0.009	7908.992	-0.004	7891.715	-0.004
24	7947.271	0.004	7928.392	-0.001	7910.264	-0.008	7927.727	-0.002	7908.945	-0.006	7890.924	0.000
25	7947.982	0.003	7928.350	-0.002	7909.478	-0.000	7928.435	0.003	7908.899	-0.005	7890.132	0.004
26	7948.695	0.004	7928.306	-0.004	7908.690	0.008	7929.135	0.002	7908.851	-0.005	7889.335	0.006
27	7949.406	0.007	7928.262	-0.003	7907.887	0.003	7929.838	0.006	7908.801	-0.005	7888.523	-0.007
28	7950.108	0.002	7928.216	-0.003	7907.085	-0.001	7930.532	0.004	7908.748	-0.006	7887.732	0.004
29	7950.818	0.006	7928.170	-0.002	7906.292	0.007	7931.226	0.004	7908.690	-0.010	7886.926	0.001
30	7951.518	0.004	7928.121	-0.002	7905.491	0.007	7931.921	0.006	7908.639	-0.004	7886.113	-0.006
31	7952.218	0.002	7928.069	-0.002	7904.685	0.006	7932.613	0.007	7908.578	-0.007	7885.313	0.000
32	7952.908	-0.007	7928.016	-0.002	7903.875	0.000	7933.297	0.003	7908.518	-0.006	7884.509	0.005
33	7953.613	0.001	7927.962	-0.003	7903.075	0.006	7933.984	0.004	7908.455	-0.007	7883.697	0.004
34	7954.304	-0.004	7927.905	-0.003	7902.270	0.010	7934.670	0.007	7908.390	-0.008	7882.884	0.003
35	7955.001	-0.000	7927.848	-0.002	7901.466	0.015	7935.348	0.003	7908.324	-0.008		
36	7955.692	-0.000	7927.787	-0.003	7900.644	0.004	7936.026	0.002	7908.258	-0.006	7881.258	0.007
37	7956.380	-0.002	7927.727	-0.002	7899.829	0.002	7936.710	0.009	7908.188	-0.006	7880.441	0.008
38	7957.068	-0.001	7927.663	-0.003	7899.012	-0.001	7937.386	0.009	7908.115	-0.007	7879.616	0.002
39	7957.750	-0.004	7927.597	-0.003	7898.199	0.002	7938.054	0.005	7908.039	-0.008		
40	7958.440	0.002	7927.531	-0.003	7897.380	0.000	7938.726	0.007	7907.964	-0.007	7877.971	0.001
41	7959.112	-0.006	7927.462	-0.003	7896.561	0.000	7939.395	0.008	7907.887	-0.006	7877.150	0.004
42	7959.791	-0.006	7927.390	-0.004	7895.740	-0.001	7940.047	-0.005	7907.810	-0.003	7876.330	0.012
43	7960.472	-0.002	7927.317	-0.005	7894.926	0.007	7940.726	0.010	7907.722	-0.009	7875.495	0.004
44	7961.146	-0.002	7927.244	-0.003	7894.094	-0.002	7941.385	0.008	7907.639	-0.007	7874.667	0.006
45	7961.815	-0.006	7927.168	-0.003	7893.268	-0.002	7942.037	0.001			7873.841	0.012

DISCUSSION

The rotational constants for the $a^3\Delta$ and $b^3\Pi$ states of HfO are provided in Tables V and VI, respectively. Due to the absence of satellite branches or transitions with $\Delta\Sigma \neq 0$ which connect spin components, we are unable to obtain a single set of molecular constants for the $a^3\Delta$ and $b^3\Pi$ states of HfO by treating each state as a Hund's case (a) state. Rather than try to fit the states together with assumed spin–orbit and spin–spin constants, it was decided to fit the components separately. The constants in Tables V and VI have been used to evaluate effective equilibrium rotational constants in each spin component. The equilibrium constants for different spin components of the $b^3\Pi$ and $a^3\Delta$ states have been provided in Tables VII and VIII, respectively. We have used the equilibrium constants of each spin component in the lower and excited states to evaluate the effective equilibrium bond length of each spin component. The bond lengths for the $a^3\Delta_1$, $a^3\Delta_2$, and $a^3\Delta_3$ spin components are 1.741943(28), 1.740432(37), and 1.738815(23) Å, whereas the corresponding values for the $b^3\Pi_{0^+}$, $b^3\Pi_{0^-}$, $b^3\Pi_1$, and $b^3\Pi_2$ spin components are 1.742475(27),

TABLE IV—*Continued*

	0-0 Band						1-1 Band					
J	Ree	O-C	Qef	O-C	Pee	O-C	Ree	O-C	Qef	O-C	Pee	O-C
46	7962.487	-0.005	7927.091	-0.003	7892.452	0.007	7942.693	0.002			7873.004	0.009
47	7963.154	-0.005	7927.015	0.001	7891.621	0.005	7943.354	0.009	7907.374	-0.006	7872.160	0.001
48	7963.829	0.003	7926.929	-0.003	7890.792	0.005			7907.282	-0.005	7871.331	0.010
49	7964.493	0.004	7926.845	-0.004	7889.963	0.008	7944.658	0.013	7907.186	-0.006	7870.488	0.005
50	7965.149	-0.001	7926.759	-0.004	7889.132	0.009	7945.306	0.015	7907.085	-0.010		
51	7965.815	0.005	7926.671	-0.004	7888.290	0.001	7945.934	-0.001	7906.988	-0.008	7868.805	0.006
52	7966.474	0.007	7926.585	-0.002	7887.461	0.008	7946.578	0.001	7906.889	-0.005	7867.964	0.010
53	7967.130	0.009	7926.492	-0.003	7886.625	0.010	7947.222	0.006	7906.785	-0.005	7867.120	0.013
54			7926.400	-0.002	7885.778	0.001	7947.857	0.006	7906.680	-0.005	7866.259	-0.001
55	7968.429	0.005	7926.308	0.001	7884.936	-0.000	7948.496	0.010	7906.570	-0.006	7865.417	0.008
56	7969.089	0.018	7926.208	-0.002	7884.085	-0.009	7949.118	0.001	7906.458	-0.008	7864.565	0.008
57	7969.722	0.006	7926.108	-0.003	7883.255	0.005	7949.756	0.011	7906.348	-0.006	7863.703	-0.000
58	7970.366	0.008	7926.007	-0.002	7882.402	-0.002	7950.374	0.003	7906.241	0.002		
59			7925.904	-0.003	7881.556	-0.001	7950.991	-0.004	7906.117	-0.005		
60			7925.800	-0.002	7880.712	0.003	7951.624	0.009	7905.995	-0.008	7861.137	0.007
61	7972.284	0.011	7925.692	-0.003	7879.852	-0.007	7952.241	0.007	7905.879	-0.002	7860.283	0.014
62	7972.911	0.006	7925.582	-0.003			7952.859	0.010	7905.747	-0.010	7859.420	0.014
63	7973.547	0.011	7925.473	-0.000			7953.466	0.004	7905.629	-0.003		
64	7974.182	0.018	7925.359	-0.002	7877.292	-0.006	7954.077	0.006	7905.491	-0.013	7857.684	0.011
65	7974.851	-0.006	7925.243	-0.002	7876.451	0.010	7954.682	0.003	7905.368	-0.005	7856.808	0.004
66			7925.127	-0.001	7875.577	-0.006	7955.281	-0.015	7905.235	-0.005	7855.947	0.013
67			7925.007	-0.000	7874.722	-0.001	7955.903	0.006	7905.097	-0.008	7855.069	0.008
68			7924.891	0.006	7873.841	-0.020	7956.498	0.002	7904.953	0.003	7854.189	0.002
69			7924.761	-0.001	7873.004	0.006	7957.090	-0.002				
70			7924.636	0.000	7872.125	-0.007						
71			7924.507	-0.000	7871.270	0.005						
72			7924.372	-0.005	7870.397	0.000						
73			7924.245	0.001	7869.530	0.003						
74			7924.107	-0.002	7868.662	0.007						
75			7923.971	-0.001	7867.765	-0.016						
76			7923.837	0.004	7866.897	-0.008						
77			7923.692	0.001	7866.027	-0.001						
78			7923.543	-0.004	7865.132	-0.017						
79			7923.401	-0.000	7864.253	-0.016						
80			7923.257	0.005								
81			7923.097	-0.005								
82			7922.948	-0.000								
83			7922.791	-0.002								
84			7922.635	-0.000								
85			7922.475	-0.001								
86			7922.312	-0.000								
87			7922.147	-0.001								

TABLE V

Spectroscopic Constants (in cm^{-1}) for the $a^3\Delta$ Spin Components of HfO

	$a\,^3\Delta_1$		$a\,^3\Delta_2$		$a\,^3\Delta_3$	
Constants	v=0	v=1	v=0	v=1	v=0	v=1
T_v	0.0	a	b	c	d	e
B_v	0.377284(9)	0.375439(12)	0.377957(13)	0.376143(12)	0.378644(7)	0.376795(11)
$10^7 \times D_v$	2.458(13)	2.216(25)	2.842(33)	2.642(22)	2.766(11)	2.573(27)
$10^{12} \times H_v$	-0.160(38)	-2.242(88)	3.42(21)	1.51(11)	-0.110(22)	-0.27(18)
$10^9 \times q_{Dv}$	-1.072(51)	1.35(13)	--	--	--	--

Note: The letters a, b, c, d and e represent the undetermined positions of v=1 ($^3\Delta_1$), v=0 ($^3\Delta_2$), v=1 ($a\,^3\Delta_2$), v=0 ($a\,^3\Delta_3$) and v=1 ($a\,^3\Delta_3$) vibrational levels, respectively.

TABLE VI

Spectroscopic Constants (in cm^{-1}) for the $b^3\Pi$ Spin Components of HfO

	$b^3\Pi_{0^+}$		$b^3\Pi_0$	
Constants	v=0	v=1	v=0	v=1
T_v	7060.5778(10)	7047.8277(11)+a	7356.1873(10)	7345.7790(10)+a
B_v	0.377080(9)	0.375289(12)	0.377188(9)	0.375391(12)
$10^7 \times D_v$	2.551(13)	2.595(22)	2.550(12)	2.587(24)

	$b^3\Pi_1$		$b^3\Pi_2$	
Constants	v=0	v=1	v=0	v=1
T_v	7375.9610(10)+b	7357.4185(10)+c	7928.8781(5)+d	7909.5052(9)+e
B_v	0.376880(13)	0.374984(11)	0.377841(7)	0.375879(11)
$10^7 \times D_v$	2.584(28)	2.532(20)	2.874(11)	2.694(23)
$10^4 \times q_v$	-5.177(11)	-5.167(9)	--	--
$10^9 \times q_{Dv}$	2.40(35)	2.31(25)	--	--

1.742219(27), 1.742816(36), and 1.740528(23) Å, respectively. In view of the Hund's case (c) tendencies which HfO displays, treating each spin component as a separate state is not unreasonable.

Edvinsson and Nylén (*40*) have mentioned in their work that they also observed very weak 0–1 and 1–0 bands associated with the $C - x_1$ subband of their $^3\Phi$–$^3\Delta$ transition, but unfortunately they did not provide the bandhead positions. We did not observe any off-diagonal vibrational bands for the $c^3\Phi$–$a^3\Delta$ transition. Therefore, even though we have observed many diagonal vibrational bands for each subband, we are unable to determine the vibrational frequencies of the states.

Although there is no theoretical work available for HfO, the electronic structure of the low-lying states can be very reliably obtained by comparing HfO with TiO and ZrO. TiO is perhaps the best characterized $3d$ transition metal oxide. All of the elec-

TABLE VII

Equilibrium Constants (in cm^{-1}) for the $a^3\Delta$ Spin Components of HfO

Constants	$a^3\Delta_1$	$a^3\Delta_2$	$a^3\Delta_3$
B_e	0.378207(12)	0.378864(16)	0.379569(10)
α_e	0.001845(15)	0.001814(18)	0.001849(14)
r_e(Å)	1.741943(28)	1.740432(37)	1.738815(23)

TABLE VIII

Equilibrium Constants (in cm^{-1}) for the $b^3\Pi$ Spin Components of HfO

Constants	$b^3\Pi_{0^+}$	$b^3\Pi_0$	$b^3\Pi_1$	$b^3\Pi_2$
B_e	0.377976(12)	0.378087(12)	0.377828(16)	0.378822(10)
α_e	0.001791(15)	0.001797(15)	0.001896(17)	0.001962(13)
r_e(Å)	1.742475(27)	1.742219(27)	1.742816(38)	1.740528(23)

tronic states observed to date are well represented by single electronic configurations (*45–47*). The ground state of this molecule has been established as the $X^3\Delta$ state arising from the $8\sigma^2 3\pi^4 9\sigma^1 1\delta^1$ electronic configuration. The lowest-energy triplet excited state of TiO is the $E^3\Pi$ state which arises from the $8\sigma^2 3\pi^4 9\sigma^1 4\pi^1$ electronic configuration. The configuration of this state can be obtained from the ground $X^3\Delta$ state by promoting the unpaired 1δ electron to the vacant 4π orbital. The $E^3\Pi$–$X^3\Delta$ transition of TiO has recently been rotationally analyzed by Simard and Hackett (*43*). The analogous $b'^3\Pi$–$a^3\Delta$ transition of ZrO, located in the near infrared at 930 nm, has also been investigated at high resolution by Phillips *et al.* (*15*). For ZrO the $a^3\Delta_1$, $a^3\Delta_2$, and $a^3\Delta_3$ spin components have been found to lie at 1099.08, 1386.99, and 1724.6 cm^{-1}, respectively, above the ground $X^1\Sigma^+$ state (*18*). A schematic energy level diagram of the observed low-lying electronic states of HfO is presented in Fig. 7. The position of the triplet manifold relative to that of the singlet manifold is not yet known for HfO. The equilibrium bond length of 1.740432(37) Å for the $a^3\Delta_2$ spin component compares with the bond lengths 1.6202 Å for the $X^3\Delta$ state of TiO and 1.7285 Å for the $a^3\Delta_2$ spin component of ZrO (1.7285 Å).

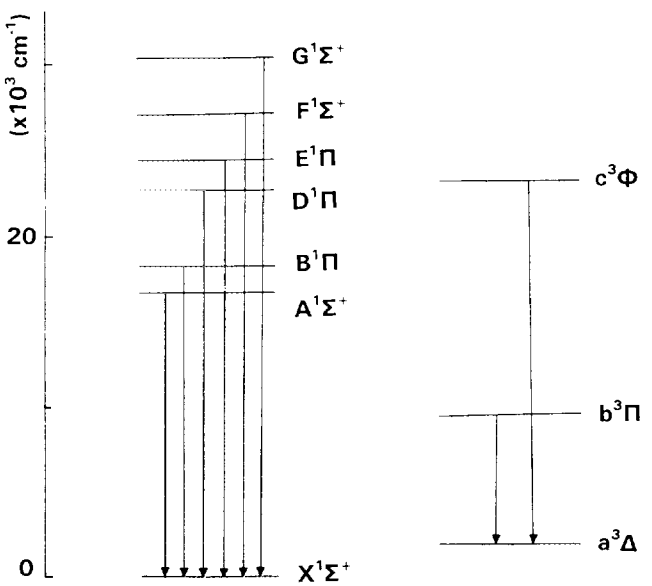

FIG. 7. A schematic energy-level diagram of the electronic states of HfO.

The ab initio calculations on TiO predict a $^3\Sigma^-$ state in the vicinity of the $E^3\Pi$ state (*45–47*). A $^3\Sigma^-$ state is also predicted for ZrO close to its $b'^3\Pi$ state (*48*) and a similar $^3\Sigma^-$ state is also possible for HfO. It is difficult to verify the existence of this state for HfO from the present work since we do not observe any extra transitions in our spectra and the transition from a $^3\Sigma^-$ state to a $^3\Delta$ state is not allowed. Presumably the Ω-doubling in the $b^3\Pi$ state is caused mainly by this $^3\Sigma^-$ state. The similarity in the HfO and ZrO bond lengths is a result of the "lanthanide contraction" of atomic radii caused by the presence of the filled $4f$ subshell in the atomic configuration of Hf.

CONCLUSION

The 400-nm to 5-μm spectral region of HfO has been investigated by Fourier transform emission spectroscopy of a hafnium hollow cathode discharge. The new bands observed in the infrared in the 6800–8000 cm^{-1} region belong to four sequences assigned as the $^3\Pi_{0^+}-^3\Delta_1$, $^3\Pi_{0^-}-^3\Delta_1$, $^3\Pi_1-^3\Delta_2$, and $^3\Pi_2-^3\Delta_3$ subbands of a new $b^3\Pi-a^3\Delta$ electronic transition. The rotational analysis of the 0–0 and 1–1 bands of each subband provides the effective equilibrium rotational constants for each spin component of the lower and excited states. The excited $b^3\Pi$ state is the analogous state to the $E^3\Pi$ state of TiO and the $b'^3\Pi$ state of ZrO.

ACKNOWLEDGMENTS

We thank J. Wagner, C. Plymate, and P. Hartmann of the National Solar Observatory for assistance in obtaining the spectra. The National Solar Observatory is operated by the Association of Universities for Research in Astronomy, Inc., under contract with the National Science Foundation. The research described here was supported by funding from the Petroleum Research Fund, administered by the American Chemical Society and the NASA Origin of the Solar System Program. Support was also provided by the Natural Sciences and Engineering Research Council of Canada.

RECEIVED: August 5, 1994

REFERENCES

1. A. J. MERER, *Annu. Rev. Phys. Chem.* **40,** 407–438 (1989).
2. D. N. DAVIS, *Astrophys. J.* **106,** 28–75 (1947).
3. H. SPINRAD AND R. F. WING, *Annu. Rev. Astron. Astrophys.* **7,** 269–302 (1969).
4. P. W. MERRILL, A. J. DEUTSCH, AND P. C. KEENAN, *Astrophys. J.* **136,** 21–34 (1962).
5. H. MACHARA AND Y. Y. YAMASHITO, *Publ. Astron. Soc. Jpn.* **28,** 135–140 (1976).
6. S. WYCKOFF AND R. E. S. CLEGG, *Mon. Not. R. Astron. Soc.* **184,** 127–143 (1978).
7. A. J. SAUVAL, *Astron. Astrophys.* **62,** 295–298 (1978).
8. D. L. LAMBERT AND R. E. S. CLEGG, *Mon. Not. R. Astron. Soc.* **191,** 367–389 (1980).
9. N. M. WHITE AND R. F. WING, *Astrophys. J.* **222,** 209–219 (1978).
10. K.-P. HUBER AND G. HERZBERG, "Constants of Diatomic Molecules," Van Nostrand-Reinhold, New York, 1979.
11. T. C. STEIMLE AND Y. AL-RAMADIN, *J. Mol. Spectrosc.* **122,** 103–112 (1987).
12. W. J. CHILDS, O. POULSEN, AND T. C. STEIMLE, *J. Chem. Phys.* **88,** 598–606 (1988).
13. B. SIMARD, A. M. JAMES, P. A. HACKETT, AND W. J. BALFOUR, *J. Mol. Spectrosc.* **154,** 455–457 (1992).
14. J. A. C. GALLAS, R. E. FRANCKE, H. P. GRIENEISEN, AND B. P. CHAKRABORTY, *Astrophys. J.* **229,** 851–855 (1979).
15. J. G. PHILLIPS, S. P. DAVIS, AND D. C. GALEHOUSE, *Astrophys. J.* **234,** 401–406 (1979).
16. P. D. HAMMER AND S. P. DAVIS, *Astrophys. J.* **237,** L51–L53 (1980).
17. P. D. HAMMER AND S. P. DAVIS, *Astrophys. J. Suppl. Ser.* **47,** 201–228 (1981).
18. S. P. DAVIS AND P. D. HAMMER, *Astrophys. J.* **332,** 1090–1091 (1988).
19. J. L. FEMENIAS, G. CHEVAL, A. J. MERER, AND U. SASSENBERG, *J. Mol. Spectrosc.* **124,** 348–368 (1987).

20. J. K. BATES AND D. M. GRUEN, *J. Mol. Spectrosc.* **78,** 284–297 (1979).
21. Y. M. HAMRICK, S. TAYLOR, AND M. D. MORSE, *J. Mol. Spectrosc.* **146,** 274–313 (1991).
22. R. SCULLMAN AND B. THELIN, *J. Mol. Spectrosc.* **56,** 64–75 (1975).
23. P. CARETTE, *J. Mol. Spectrosc.* **140,** 269–279 (1990).
24. R. D. SUENRAM, F. J. LOVAS, G. T. FRASER, AND K. MATSUMURA, *J. Chem. Phys.* **92,** 4724–4734 (1990).
25. R. J. ACKERMAN, E. G. RAUH, AND R. J. THORN, *J. Chem. Phys.* **65,** 1027–1031 (1976).
26. A. N. SAMOILOVA, Y. M. EFREMOV, AND L. V. GURVICH, *J. Mol. Spectrosc.* **86,** 1–15 (1981).
27. W. J. BALFOUR AND R. S. RAM, *J. Mol. Spectrosc.* **100,** 164–173 (1983).
28. W. J. BALFOUR AND R. S. RAM, *Can. J. Phys.* **62,** 1524–1537 (1884).
29. W. J. BALFOUR AND R. S. RAM, *J. Mol. Spectrosc.* **105,** 360–368 (1984).
30. C. I. FRUM, R. ENGLEMAN, JR., AND P. F. BERNATH, *J. Mol. Spectrosc.* **150,** 566–575 (1991).
31. R. S. RAM AND P. F. BERNATH, *J. Mol. Spectrosc.* **155,** 315–325 (1992).
32. R. S. RAM, C. N. JARMAN, AND P. F. BERNATH, *J. Mol. Spectrosc.* **160,** 574–584 (1992).
33. A. S. KING, *Astrophys. J.* **70,** 105–113 (1929).
34. R. W. SHAW AND H. C. KETCHAM, *Phys. Rev.* **45,** 753 (1934).
35. S. G. KRISHNAMURTHY, *Proc. Phys. Soc. London A* **64,** 852 (1951).
36. A. GATTERER, J. JUNKES, E. W. SALPETER, AND B. ROSEN, "Molecular Spectra of Metallic Oxides," Specola Vaticana, 1957.
37. W. WELTNER AND D. MCLEOD, *J. Phys. Chem.* **69,** 3488–3500 (1965).
38. E. A. RAUH AND R. J. ACKERMANN, *J. Chem. Phys.* **60,** 1396–1400 (1974).
39. R. J. ACKERMANN AND E. G. RAUH, *J. Chem. Phys.* **60,** 2266–2271 (1974).
40. G. EDVINSSON AND CH. NYLÉN, *Phys. Scr.* **3,** 261–266 (1971).
41. J. G. PHILLIPS, *Astrophys. J.* **114,** 152–162 (1951).
42. A. LAGERQVIST, U. UHLER, AND R. F. BARROW, *Ark. Fys.* **8,** 281–293 (1954).
43. B. SIMARD AND P. A. HACKETT, *J. Mol. Spectrosc.* **148,** 128–135 (1991).
44. L. J. LAUCHLAN, J. M. BROM, AND H. P. BROIDA, *J. Chem. Phys.* **65,** 2672–2678 (1976).
45. D. E. CARLSON AND C. MOSER, *J. Chem. Phys.* **46,** 35–46 (1967).
46. C. W. BAUSCHLICHER, P. S. BAGUS, AND C. J. NELIN, *Chem. Phys. Lett.* **101,** 229–234 (1990).
47. J. M. SENNESAL AND J. SCHAMPS, *Chem. Phys.* **114,** 37–42 (1987).
48. S. R. LANGHOFF AND C. W. BAUSCHLICHER, *J. Chem. Phys.* **89,** 2160–2169 (1988).
49. S. R. LANGHOFF AND C. W. BAUSCHLICHER, *Astrophys. J.* **349,** 369–375 (1990).
50. B. A. PALMER AND R. ENGLEMAN, "Atlas of the Thorium Spectrum" (Los Alamos National Laboratory, Los Alamos, 1983). Unpublished.
51. C. R. BRAZIER, R. S. RAM, AND P. F. BERNATH, *J. Mol. Spectrosc.* **120,** 381–402 (1986).
52. J. M. BROWN AND A. J. MERER, *J. Mol. Spectrosc.* **74,** 488–494 (1979).